ARTICLE

Nanosecond Rapid Crystallization of Water Induced by Quartz Glass under Dynamic Compression

Yong-hong Li[a,b*], Ning-chao Zhang[b], Wen-peng Wang[b], Fu-sheng Liu[b]

a. Department of Physics and Electronic Engineering, Yuncheng University, Yuncheng 044000, China
b. Key Laboratory of High Pressure Science and Technology, Southwest Jiaotong University, Chendu 610031, China

(Dated: Received on September 25, 2014; Accepted on November 25, 2014)

Optical transmission characteristics of water between quartz glass under shock compression are *in situ* observed by using the technique of missile-borne light source. Through these transmission properties, the phase transition of liquid water is studied. The experimental results show that liquid water exhibits transparency decline phenomenon when the pressure is lower than 2 GPa under shock compression process, and the transparency variation is related to the existence of quartz glass. So, the transparency decline is attributed to a quartz-induced freezing phenomenon of water.

Key words: Water, Quartz glass, Shock wave, Phase transition

I. INTRODUCTION

Water, one of the most common natural substances on earth, is an important resource for the survival of all life, including humans. It is the most important part of living organisms, and known as the "origin of life". In addition, water has many unusual physical and chemical properties, making it a subject of widespread concern in the academic community. Some new characteristics of water are continuously being discovered and reported.

A very important field in water research is water structure transition. An important experimental method for studying the material structure transition involves changing the system pressure and temperature conditions. Pressure obtained in the experiment can be divided into static pressure (mechanical extrusion) and dynamic pressure (shock wave). For static pressure experiments, the investigation of phase transition of water was first carried out by Bridgman [1]. From then on, these studies were continuously conducted [2−13]. Studies on shock waves were performed to determine whether they can cause water transition under shock compression conditions. Compared with traditional static high-pressure loading, shock wave loading has higher loading rate, shorter relaxation time, and other advantages. The phase transition from α to ε of iron was first discovered in shock compression experiment [14].

In 1957, Walsh *et al.* first engaged in a study of phase transition of water [15]. Kormer [16] and Rybakov [17] also performed many experiments on shock solidification of water. However, due to experimental condition limitations, experimental data of water freezing under shock compression are inadequate. Some experimental pieces of evidence are only limited in free surface velocity historical observations or Hugoniot data nonlinear measurement. Due to technical difficulties in diagnosis, the study on liquid shock solidification was limited [18].

The testing technology used in shock wave experiments has recently achieved great progress. Transmission spectra [19−23] and Raman spectra [24−26] are used in shock wave loading experiments to measure phase transition of liquid substance. Thus, phase transition under shock compression has been a subject of great attention. Shock wave loading will cause high temperature rise, which is not conductive to shock solidification of liquid substance. Multiple shock and magnetic quasi-isentropic compression techniques have been adopted. For example, Dolan *et al.* adopted multiple shock method in gas gun experiments to determine whether there was water crystallization by changing the transmitted light intensity and obtained the change in characteristics of water liquid−solid phase transition [19−21]. They made a breakthrough in the study on transformation of water under shock compression, and found that when liquid water was under multiple shock compression to solid phase (ice VII) in the super-cooled state, it achieved rapid crystallization. However, crystallization occurred only with the use of quartz window containing Si element. When sapphire, which does not contain Si element, was used as the optical window, no change in the structure of water in less than 5 GPa of the whole compression process was observed.

At present, the direct basis for water liquid−solid phase transition is only limited to the results reported

*Author to whom correspondence should be addressed. E-mail: liyonghong02721227@163.com

by Dolan *et al* that silicon glass was conductive to the crystallization phase transition of water, indicating the existence of some kind of interaction between them. If water is affected by outside forces, then icing conditions will change as well. For example, Choi *et al.* [27] found that the icing of water occurred at room temperature environment in the electric field. In the present study, we present the following questions: (i) under the effect of silicon glass, does the freezing phase change still need super-cooling? If quartz has an effect on the freezing process of water, the super-cooled phase transition reported by Dolan *et al.* [19] is debatable; and (ii) is the effect of silicon glass on water indirect or direct? A set of missile-borne light source *in situ* testing techniques were designed in a one-stage light gas gun, and multiple shock was used to do further research on shock-induced phase transition of water.

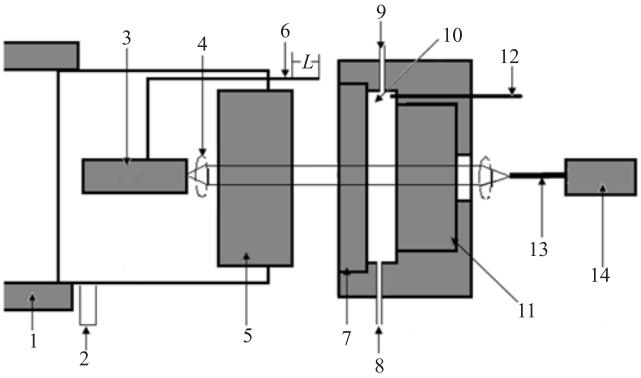

FIG. 1 Schematic view of the experiment. 1: Gun tube, 2: magnetic measuring speed device, 3: light source, 4: lens, 5: flyer, 6: tigger, 7: baseplate, 8: entrance, 9: exit, 10: sample, 11: window, 12: thermocouple, 13: optical fiber, 14: test system.

II. EXPERIMENTS

Figure 1 shows the schematic diagram of the experimental apparatus that mainly consist of the gun tube for the launching projectile, the projectile, the target, and the test system. The projectile is launched by a one-stage light gas gun. After acceleration by the gun tube, the speed is measured using electromagnetic induction technique. One characteristic of the *in situ* testing technology is to arrange a pulsed light source in the projectile axis to observe the transparency of transparent samples in the target in the loading process. The light source is a small 0.5 mW LED. The working voltage is 4.5 V, with wavelength of 650±10 nm. The front end of the light source is equipped with a lens that can adjust the light beam diameter≤2 mm. A probe tip is higher than the flyer, with the distance of L. The target is mainly composed of the flyer (ø30 mm×12 mm), baseplate (ø40 mm×2.5 mm), and window (ø30 mm×10 mm). The material is transparent quartz glass, with density ρ=2.20 g/cm^3 and wave velocity C_l=5.95 km/s. The input and export on the target are connected to the externally circulating water (not in figure), which can change the initial temperature at any time. The initial value of the temperature is measured using a thermocouple. The test system consists of an oscilloscope and a computer. After acceleration, the projectile is in collision with the baseplate. First, the probe gets into contact with the target and triggers the light source. The light goes through the flyer, baseplate, and window. It is collected by fiber and is delivered to the test system, and then recorded by the oscilloscope. After the light source becomes stable, the front end flyer collides with the baseplate and generates a shock wave on the interface. The shock wave is then spread to the sample for loading. It also transfers shock wave into the flyer to load the flyer. The sample in the experiment is thinner, so the shock wave will be reflected back and forth between the baseplate and the window for the multiple shock loading, stepping up the pressure in the sample. The sample pressure, baseplate and window achieve balance. At the same time, the pressure in a sample also reaches a peak. The flyer thickness (12 mm) selection is much larger than the baseplate thickness (2.5 mm), so the test in the present work may neglect the influence of the unloading wave on experimental data.

The shock impedance matching technique is used to determine the shock pressure and particle velocities of each multiply shocked states during the process of compression. Figure 2 shows the calculation details in P-u plane. The numbers in Fig.2 indicate the points (u_i, P_i) of the ith shock states, which can be solved out by finding the crossing points between Hugoniots of water and that of baseplate, and between Hugoniots of water and that of window [28]. In our experiments, the shock velocity keeps its longitude speed because the compression of quartz does not reach its elastic limit, and the changes of Hugoniots of related substances during multiple shock processes are neglected by consideration of the weak compression conditions.

For baseplate, its Hugoniot is described by Eq.(1):

$$P = \rho_{0q}(W - D_{\rm e})\,(W - u) \tag{1}$$

where P, ρ_{0q}, u, $D_{\rm e}$, and W denote the pressure, density, particle velocity, shock wave velocity, and projectile velocity of the baseplate, respectively.

For window, its Hugoniot is described by Eq.(2):

$$P = \rho_{0q} D_{\rm e} u \tag{2}$$

For water, the Hugoniots of ith shock compression in D-u plane are given by Eq.(3) [29, 30]:

$$D = 1.44 + 2.16u - 0.19u^2 \tag{3}$$

In our multiple shock calculation, the Hugoniots in P-u plane are given in two different forms.

DOI:10.1063/1674-0068/28/cjcp1409160

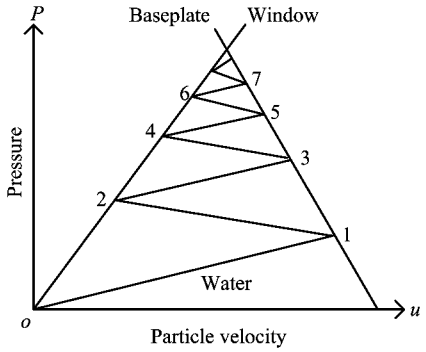

FIG. 2 Principle of shock impedance-matching techniques. "baseplate", "window", and "water" respectively represent the Hugoniot of quartz baseplate, quartz window, and water sample.

For i=odd:

$$P_{\mathrm{H}}^{i}(u) = p_{i-1} + \rho_{i-1}[1.44 + 2.16(u - u_{i-1}) - 0.19(u - u_{i-1})^2](u - u_{i-1}) \quad (4)$$

For i=even:

$$P_{\mathrm{H}}^{i}(u) = p_{i-1} + \rho_{i-1}[1.44 + 2.16(u_{i-1} - u) - 0.19(u_{i-1} - u)^2](u_{i-1} - u) \quad (5)$$

The later form just describes the mirror inversion line of the former.

The specific volume of each multi-shock states is calculated by Eq.(6), and the shock temperature $T_{\mathrm{H}}^{i}(V)$ is calculated by Eq.(7) [31]:

$$V_i = V_{i-1}\left(1 - \frac{u_i - u_{i-1}}{D_i - u_{i-1}}\right) \quad (6)$$

$$\frac{\mathrm{d}T_{\mathrm{H}}^{i}}{\mathrm{d}V} + \frac{\gamma}{V}T_{\mathrm{H}}^{i} = \frac{1}{2C_V}\left[P_{\mathrm{H}}^{i} + (V_{i-1} - V)\frac{\mathrm{d}P_{\mathrm{H}}^{i}}{\mathrm{d}V}\right] \quad (7)$$

where D and V denote particle velocity and the shock wave velocity of the sample respectively, and the subscript i represents ith-shock.

In the calculations, we ignore the change of the specific heat $C_V(V)$ of water, which is taken as the parameters, the Gruneisen coefficient $\gamma(V)$ [32] is:

$$\gamma(V) = 0.52 + 0.0589\eta + 36.949\eta^2 \quad (8)$$

$$\eta = \frac{\rho}{\rho_0} - 1 \quad (9)$$

where ρ_0=0.998 g/cm^3, η and ρ_0 are the normal water density values.

III. RESULTS AND DISCUSSION

Five multiple shock experiments on the water samples were carried out. The experimental parameters, including projectile velocity W, initial thickness of samples H, initial temperature T_0, are shown in Table I, the pressure P, temperature T, and time t are shown in Table II.

TABLE I Experimental parameters including projectile velocity W, initial thickness of samples H, initial temperature T_0.

Experiment	W/(m/s)	H/mm	T_0/K
1	167	0.60	285
2	247	0.52	285
3	416	0.49	285
4	498	0.64	328
5	540	0.67	285

Figure 3 shows variation of the transmission characteristics and pressure of the sample water with time under shock compression process in experiment 1, 2, 3, and 4. In each diagram, the upper part is the loading variation in the process of compression with time as the abscissa and pressure as the ordinate, the lower part is the change of transmission with respect to time. Transmission is the ratio of light intensity during sample compression I to light intensity before compression I_0. Zero time is for the moment the shock wave enters the sample. F location is for the arrival time of the shock wave produced by flying plate collision with the baseplate.

For experiment 1, from the first to the fifth shock compression, water transmission did not change significantly with the pressure increase from 0.26 GPa to 0.91 GPa. Thus, the sample water in experiment 1 was in a transparent liquid state and maintain good transparency, as shown in Fig.3(a). Figure 3 (b)−(d) are the transmission variation characteristics and pressure change of experiments 2, 3, and 4, respectively. The curves show that transmission declines under shock compression. The transmission variation in experiments 2, 3, and 4 all occur at about dozens of nanoseconds after the fourth, second, and third shock compressions, respectively. The pressure and temperature conditions for 2, 3, and 4 transmission changes are 1.28 GPa at 340 K (state A), 1.62 GPa at 345 K (state B), and 2.74 GPa at 420 K (state C), respectively (Table II). The three states A, B, and C, and the locations of the shock compression process of experiments 2, 3, and 4 in the phase diagram of water are shown in Fig.4. The three states are still in the liquid phase in the phase diagram. In the whole shock compression process of experiments 2 and 4, the thermodynamic state remains in the liquid region. However, Dolan *et al.* [19] reported that only when liquid water was compressed to 2 GPa into the solid phase region, which was in the super-cooled state that induced crystalline phase transition, did transmission variation occur. However, experimental results show that in shock compression, transmission variation occurs even when it does not reach the crystalline phase transition conditions. Moreover,

DOI:10.1063/1674-0068/28/cjcp1409160

TABLE II Sample of water pressure (P in GPa), temperature (T in K), and time (t in ns) calculation results.

Expt.	The first shock			The second shock			The third shock			The fourth shock			The fifth shock		
	$P1$	$T1$	$t1$	$P2$	$T2$	$t2$	$P3$	$T2$	$t3$	$P4$	$T4$	$t4$	$P5$	$T5$	$t5$
1	0.26	300	339	0.50	311	253	0.70	318	211	0.83	322	191	0.91	324	173
2	0.42	308	261	0.80	324	194	1.08	334	165	**1.28**	**340**	**150**	1.39	343	142
3	0.78	329	221	**1.62**	**345**	**128**	2.18	355	97	2.45	358	87	2.56	361	83
4	0.98	383	270	2.08	410	147	**2.74**	**420**	**110**	3.02	424	100	3.12	425	97
5	1.10	337	275	2.33	362	146	3.03	371	110	3.32	374	99	3.42	376	95

Note: The bold numbers show the transmission change at the three states.

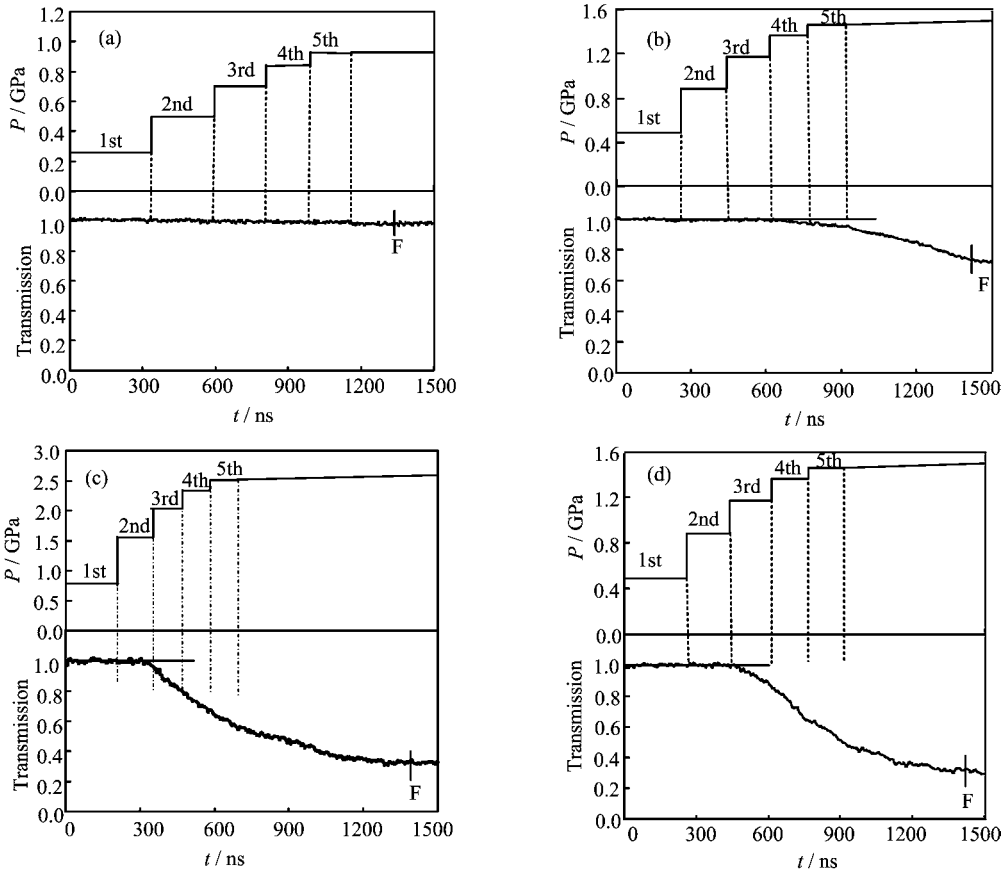

FIG. 3 Transmission and the pressure change in different experiments. (a) experiment 1, (b) experiment 2, (c) experiment 3, and (d) experiment 4.

in the process of changing shock compression (experiment 3 in Fig.4) from the third to the fourth (across the liquid−solid boundary), the transmission curve tendency has no obvious change in Fig.3(c), as it has no inflection point. If the transmission variation is determined by the thermodynamic reason, the trend of transmission curve of experiment 3 should be different across the phase boundary.

To find the cause of the transmission decrease, we designed the following experiment: place the transparent organic glass film in close contact with the quartz glass interface (the interface in which the baseplate and the window go in contact with water) to separate the sample in the chamber with the quartz glass sample chamber. The transmission variation features are shown in Fig.5. In multiple shock compression process, it has good transparency in the range of 0−3.42 GPa. Consequently, the water transparency decline is closely related to whether or not it is in direct contact with the quartz glass.

The thermodynamic state remains at the liquid region and does not enter the ice phase when transparency becomes worse under shock compression, so super-cooled condition cannot be used to explain the

DOI:10.1063/1674-0068/28/cjcp1409160

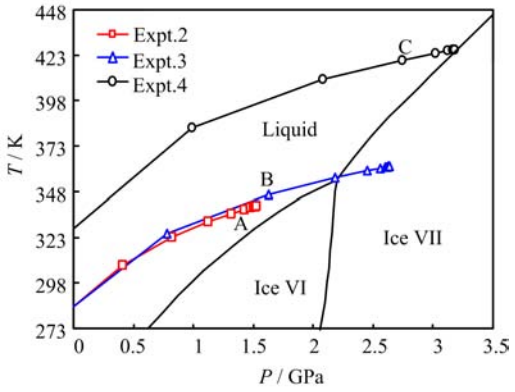

FIG. 4 Phase diagram of water and the shock compression process of experiments 2, 3, and 4.

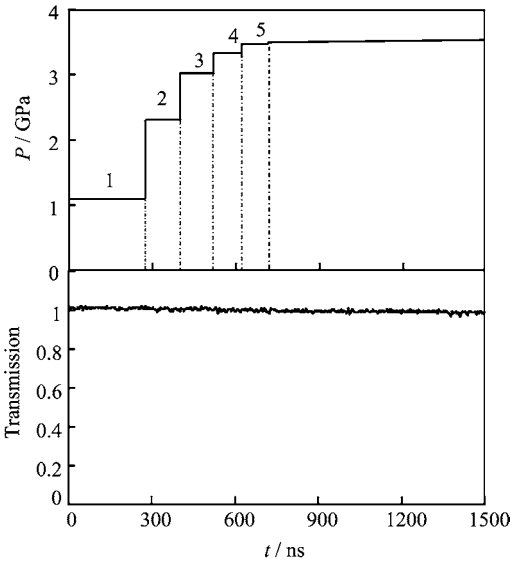

FIG. 5 Transmission and the pressure change of water sample in experiment 5.

liquid−solid transition and transparency decline. Furthermore, the transparent variation is closely related to the existence of quartz glass; that is, there is an interaction between quartz and water. Ostroverkhov *et al.* [33, 34] and Asay *et al.* [35] reported that when the quartz glass went in contact with water, oxygen in quartz and hydrogen in water formed a hydrogen bond due to the electrode, which resulted in an ice-like structure, because some water molecules were arranged in an orderly manner on the quartz surface. Hydrogen bonds played a role of great importance in the formation of ice. That is to say, they connect the water molecules to form a space structure. Before the shock compression experiments, water molecules with ice-like structure exist on the quartz glass surface. The structure is like a nucleation seed distributed at the interface, which has the seeds of the phase transition. With the effect of the shock wave as a driving force, it will grow and result in partially uneven water. A portion of the transmitted light is scattered and weakened, so the transparent rate decreases. When the water and quartz glass interfaces are isolated, phase change will not occur because it does not have the nucleation seed. Thus, in experiment 5, transmission variation is not observed, as shown in Fig.5. Based on this above analysis, water transmission droplets should be made by quartz glass-induced water molecule solidification.

IV. CONCLUSION

Using ammunition source *in situ* testing techniques, the transmission characteristics of water between quartz glass under shock compression on the light-gas gun have been observed. We obtain new understanding as follows: (i) in shock compression process, transparency difference of water can occur under 2 GPa, which does not reach super-cooled conditions; (ii) in shock compression, the transmission decline of the water sample remains similar to that of the thermodynamic state changing from liquid to solid; and (iii) transparent water decline is related to quartz glass existence. Based on these results, the research findings of Dolan *et al.* [19] that the transparency drops of water occur only above 2 GPa and that the drops are attributed to supercooled crystallization, are not accurate. The transparent variation of water between quartz glass in the process of shock compression is due to the quartz glass-induced water phase transition, not the occurrence of liquid−solid phase transition. Water and quartz are common and important materials on earth, so the results in this work are of value to geology.

V. ACKNOWLEDGMENTS

This work was supported by the National Natural Science Foundation of China (No.108741414), the Science and Technology Innovation Project of Shanxi Province Higher Education (No.2013153), and the Yunchen University Research Project (No.YQ-2014012).

[1] P. W. Bridgman, J. Chem. Phys. **5**, 964 (1937).
[2] A. Polian and M. Grimsdicth, Phys. Rev. B **27**, 6409 (1983).
[3] I. M. Chou, J. G. Blank, A. F. Goncharov, H. K. Mao, and R. J. Hemley, Science **281**, 809 (1998).
[4] O. Mishima and H. Stanley, Nature **392**, 164 (1998).
[5] O. Mishima, Phys. Rev. Lett. **85**, 334 (2000).
[6] C. A. Tulk, C. J. Benmore, J. Urquidi, D. D. Klug, J. Neuefeind, B. Tomberli, and P. A. Egelstaff, Science **297**, 1320 (2002).
[7] T. Kawamoto, S. Ochiai, and H. J. Kagi, J. Chem. Phys. **120**, 5867 (2004).
[8] F. F. Li, Q. L. Cui, Z. He, T. Cui, J. Zhang, Q. Zhou, and G. T. Zou, J. Chem. Phys. **123**, 174511 (2005).

DOI:10.1063/1674-0068/28/cjcp1409160

[9] G. W. Lee, W. J. Evans, and C. K. Yoo, Phys. Rev. B **74**, 134112 (2006).
[10] G. P. Johari and O. Andersson, Phys. Rev. B **73**, 094202 (2006).
[11] C. U. Kim, B. Barstow, M. W. Tate, and S. M. Gruner, Nat. Acad. Sci. **106**, 4596 (2009).
[12] K. Reviews, Rev. Mineral. Geochem. **71**, 315 (2010).
[13] D. Ehre, E. Lavert, M. Lahav, and L. Lubomirsky, Science **327**, 672 (2010).
[14] Z. P. Tang, *Skock Induced Phase Transition*, Beijing: Science Press, 223 (2008).
[15] J. M. Walsh and M. H. Rice, J. Chem. Phys. **26**, 815 (1957).
[16] S. B. Kormer, Sov. Phys. Uspekhi **11**, 229 (1968).
[17] A. P. Rybakov, J. Appl. Mech. Tech. Phys. **37**, 629 (1996).
[18] G. E. Duvall and R. A. Graham, Rev. Mod. Phys. **49**, 561 (1977).
[19] D. H. Dolan and Y. M. Gupta, Chem. Phys. Lett. **374**, 608 (2003).
[20] D. H. Dolan and Y. M. Gupta, J. Chem. Phys. **121**, 9050 (2004).
[21] D. H. Dolan, M. D. Knudson, C. A. Hall, and C. Deeney, Nat. Phys. **3**, 339 (2007).
[22] Y. H. Li, W. P. Wang, N. C. Zhang, and F. S. Liu, Sci. Sin. Phys. Mech. Astron. **43**, 1035 (2013).
[23] W. P. Wang, F. S. Liu, and N. C. Zhang, Acta Phys. Sin. **63**, 126201 (2014).
[24] A. Matsuda, K. Kondo, and K. G. Nakamura, J. Chem. Phys. **124**, 054501 (2006).
[25] S. Root and Y. M. Gupta, J. Phys. Chem. **113**, 1268 (2009).
[26] B. J. Zhao, F. S. Liu, and N. C. Zhang, Chin. Phys. Lett. **30**, 030701 (2013).
[27] E. M. Choi, Y. H. Yoon, S. Lee, and H. Kang, Phys. Rev. Lett. **95**, 085701 (2005).
[28] M. J. Zhang, F. S. Liu, C. L. Tian, and Y. Y. Sun, Chin. Phys. Lett. **23**, 2190 (2006).
[29] M. H. Rice, J. Chem. Phys. **26**, 824 (1957).
[30] K. Nagayama, Y. Mori, and K. Shimada, J. Chem. Phys. **91**, 476 (2002).
[31] W. H. Tang and N. Q. Zhang, *Equation of State Theory and Computational Introduction*, Changsha: National University of Defense Technology Press, 273 (1999).
[32] A. C. Mitchell and W. J. Nellis, J. Chem. Phys. **76**, 6273 (1982).
[33] V. Ostroverkhov, G. A. Waychunas, and Y. R. Shen, Phys. Rev. Lett. **94**, 046102 (2005).
[34] V. Ostroverkhov, G. A. Waychunas, and Y. R. Shen, Chem. Phys. Lett. **386**, 144 (2004).
[35] D. B. Asay and S. H. Kim, J. Phys. Chem. B **109**, 16760 (2005).

DOI:10.1063/1674-0068/28/cjcp1409160